

ES-ENAS: Combining Evolution Strategies with Neural Architecture Search at No Extra Cost for Reinforcement Learning

Xingyou Song^{*1}, Krzysztof Choromanski^{1,2}, Jack Parker-Holder³, Yunhao Tang², Daiyi Peng¹, Deepali Jain¹, Wenbo Gao⁴, Aldo Pacchiano⁵, Tamas Sarlos¹, Yuxiang Yang⁶
¹Google, ²Columbia University, ³Oxford University, ⁴Waymo, ⁵UC Berkeley, ⁶University of Washington

ABSTRACT

We introduce ES-ENAS, a simple neural architecture search (NAS) algorithm for the purpose of reinforcement learning (RL) policy design, by combining Evolutionary Strategies (ES) [30, 40] and Efficient NAS (ENAS) [36, 54, 61] in a highly scalable and intuitive way. Our main insight is noticing that ES is already a distributed blackbox algorithm, and **thus we may simply insert a model controller from ENAS into the central aggregator in ES and obtain weight sharing properties for free**. By doing so, we bridge the gap from NAS research in supervised learning settings to the reinforcement learning scenario through this relatively simple marriage between two different lines of research, and are **one of the first to apply controller-based NAS techniques to RL**. We demonstrate the utility of our method by training combinatorial neural network architectures for RL problems in continuous control, via edge pruning and weight sharing. We also incorporate a wide variety of popular techniques from modern NAS literature, including multiobjective optimization and varying controller methods, to showcase their promise in the RL field and discuss possible extensions. We achieve > 90% network compression for multiple tasks, which may be special interest in mobile robotics [15] with limited storage and computational resources.

1 INTRODUCTION

Neural network architectures are the basic building blocks of modern deep learning, as they determine the inductive biases that models will use to process information and make predictions. Normally, these building blocks are hand-designed using human intuition and priors, such as convolutional layers which are based on the principle of visual locality. Unfortunately, finding the right architecture using e.g. the best possible combination of convolutions, can sometimes be a very tedious and laborious task, which requires training multiple models iteratively. Neural architecture search (NAS) [61], however, seeks to automate this process to both reduce human labor as well as find optimal architectures that humans may overlook. NAS has been successfully applied to designing model architectures in fields ranging from image classification [61] to language modeling [43], and has even been applied to algorithm search [38]. However, surprisingly, one field which has *not* seen relative popularity with NAS is *reinforcement learning* (RL).

While some variants of NAS specifically mix in the optimization process with the model, for example Differentiable Architecture Search [28], in most cases, the objective is treated as a blackbox function $f: \mathcal{M} \rightarrow \mathbb{R}$ where \mathcal{M} is a combinatorial, discrete search

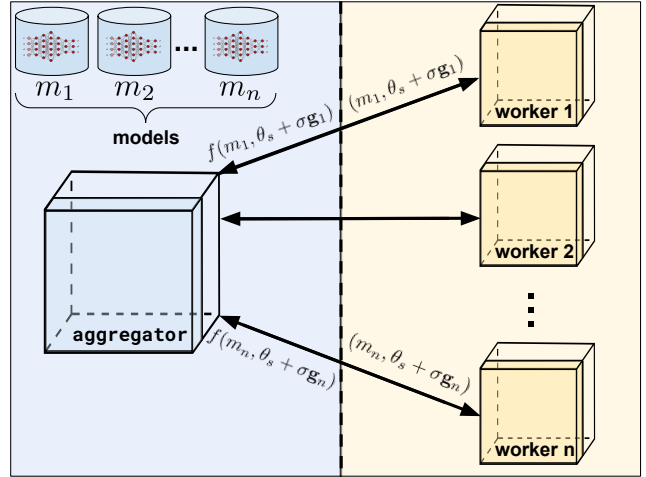


Figure 1: Figure representing our aggregator-worker pipeline, where the aggregator proposes models m_i in addition to a perturbed input $\theta_s + \sigma_{g_i}$, and the worker the computes the objective $f(m_i, \theta_s + \sigma_{g_i})$, which is sent back to the aggregator. Both the training of the weights θ_s and of the model-proposing controller p_ϕ rely on the number of worker samples to improve performance.

space representing potential components of a model architecture, and the objective is the accuracy of the model once trained to convergence.

This blackbox framework is exploited in the original NAS paper [61], where a central *controller*, first introduced as a RNN-based Pointer Network [54], parameterizes the search space \mathcal{M} with a distribution p_ϕ via neural network parameters ϕ , and proposes candidate architectures, i.e. *child models* $m \in \mathcal{M}$ to obtain objectives from which to train ϕ via policy gradient.

Further uses of this blackbox optimization framework have been explored in NASBench [58] which stores a database of pretrained model accuracies allowing fast querying of the objective function, and PyGlove[35] which programmatically attempts to decouple the search space, optimizer, and the objective function. This has led to vast literature on blackbox optimizers for NAS search spaces, such as methods to apply Bayesian Optimization [14] for NAS [55], as well as using classical *true* evolutionary methods such as NEAT [48] and Regularized Evolution [37].

However, one caveat is the lack of efficiency of such methods, as they summarize an entire model’s training run (which could take hours to days) as simply a single scalar objective, which may be problematic when there is a lack of computational resources.

^{*}Correspondence to xingyousong@google.com.

Code: github.com/google-research/google-research/tree/master/es_enas.

Efficient Neural Architecture Search [36] addresses this issue by applying weight sharing across all child models, and DARTS converts a single model into a differentially customizable one to reduce the number of completely new model instantiations. Such methods unfortunately can require significant changes in program logic, and are by default not used when there is abundance of compute resources available, such as in an industrial research lab [50, 51]. By standardizing the objective function, NASBench [58] further avoids various complications with efficient NAS methods, and encourages the community to instead only focus on blackbox optimization techniques.

Thus, we observe a natural tradeoff in NAS: *simplicity vs efficiency*. Framing NAS in the blackbox optimization setting allows very fast changes to the blackbox algorithm, but requires extensive computational resources for many tasks outside of the NASBench setting. Using techniques which exploit prior knowledge of the task can reduce the computational overhead, but requires extensive modifications to training pipelines - for instance, ENAS requires a very nonstandard computation graph, due to its need to define a global shared weight system.

However to the best of our knowledge, there also is a lack of work applying (efficient) neural architecture search methods to RL policies. We hypothesize this is due to a few reasons. One reason partially is because unlike SL, RL policies are usually quite small and thus do not require a search space involving large convolutional modules as in the case for image classification. However, we show that the search space for RL policies can still be quite combinatorial, by examining search spaces ranging from partitionings to edge prunings in our work. Another reason is due to RL possessing significantly different training infrastructure than supervised learning, as large-scale distributed on-policy and off-policy algorithms both require notions of replay buffers and the use of multiple actors and critics as CPUs, and a central worker such as a GPU for training.

One such rather conceptually simple RL algorithm is Evolutionary Strategies (ES) [40], also known as Augmented Random Search (ARS) [30, 31], which has been applied successfully to multiple domains such as Atari games, and especially in robotics due to its ability to train stable deterministic policies in continuous control tasks. ES effectively sidesteps notions of replay buffers, etc. and simply treats an agent’s total reward as a blackbox (and potentially non-differentiable) objective $f(\theta)$. This allows flexibility in the types of neural network architectures used, especially for RL problems, as certain classes of combinatorial policies, which would require special operations for backward passes, are normally difficult to implement in frameworks such as Tensorflow or Pytorch. The ES algorithm estimates a Gaussian smoothed gradient of the objective, by using multiple CPU workers to evaluate the objective.

What follows on how to combine NAS with ES should therefore be intuitive, as they are both *blackbox algorithms* and use very similar distributed workflows. Our key observation is that **ES and ENAS can naturally be combined in a highly scalable but conceptually straightforward way by simply introducing a NAS controller into the central aggregator in ES**, and appending the proposed model string with the preexisting model weights during message passing from the aggregator to the workers. **In**

doing so, we are one of the first to apply popular controller-based NAS techniques to the field of RL. A visual representation of our algorithm can be found in Fig. 1.

In terms of computational costs, to give context, vanilla NAS [61] for classical supervised learning setting (SL) requires a large population of 450 GPU-workers (“child models”) all training one-by-one, which results in many GPU-hours of training. ENAS [36] uses weight sharing across multiple workers to avoid training classifiers from scratch, and can reduce the requirement for computational resources at the cost of increasing the complexity of implementation due to the shared weight mechanism. **Our method solves both issues (training time and controller sample complexity) by leveraging a large population of much-cheaper CPU workers, on the order of hundreds to thousands, thus increasing the effective batch-size of the controller, while also training the workers simultaneously via ES.** This setup is not possible in SL, as a single CPU cannot train a large image-based classifier in practice. We thus introduce the ES-ENAS algorithm, which requires no extra computational resources and is applicable for a wide variety of RL use-cases.

2 BACKGROUND AND PRELIMINARIES

2.1 Network Architecture Search

The subject of this paper can be put in the larger context of Neural Architecture Search (NAS) algorithms which recently became a prolific area of research with already voluminous literature (see: [12] for an excellent survey). Interest in NAS algorithms started to grow rapidly when it was shown that they can design state-of-the-art architectures for image recognition and language modeling [61]. More recently it was shown that NAS network generators can be improved to sample more complicated connectivity patterns based on random graph theory models such as Erdos-Renyi, Barabasi-Albert or Watts-Strogatz to outperform human-designed networks, e.g. ResNet and ShuffleNet on image recognition tasks [57].

The foundation of our algorithm for learning policy network structure is the class of ENAS methods [36], and more broadly, controller-based methods [61]. To present our algorithm, we thus need to first describe this class. ENAS algorithms are designed to efficiently construct neural network architectures, which are usually combinatorial-flavored optimization problems with exponential-size domains, by sharing model weights across child models, thus preventing the need to completely retrain every child model from scratch. This weight sharing technique is justified in [36] due to the transferrability of weights across different architectures seen in previous literature.

More formally, a child model can be represented by its model m and its particular weights θ . In ENAS, a θ_s is *shared* across workers, whereas in the original NAS, the final objective $f(m)$ is defined only after the model converges during training. If $f(m, \theta_s)$ is the objective value (which is normally accuracy in the supervised learning setting, but as we discuss later, can also be total rewards of a policy in a reinforcement learning environment), then when using a RNN-based controller with parameters ϕ , the smoothed objective $J(\phi) = \mathbb{E}_{m \sim p_\phi} [f(m; \theta_s)]$ can be optimized by estimating the *policy*

gradient:

$$\nabla_{\phi} J(\phi) = \nabla_{\phi} \mathbb{E}_{m \sim p_{\phi}} [f(m, \theta_s)] \approx \frac{1}{n} \sum_{i=1}^n f(m_i, \theta_s) \nabla_{\theta_s} \log p_{\phi}(m) \quad (1)$$

where $\log p_{\phi}(m)$ is the log-probability of the controller for selecting m , and thus $\phi \leftarrow \phi + \eta_{pg} \nabla_{\phi} J(\phi)$ is updated with the use of the REINFORCE algorithm [56], or other policy gradient such as algorithms such as PPO [41].

Recent work such as with AmeobaNets [37] have also shown that evolutionary controllers similar to NEAT [48], termed *Regularized Evolution* (Reg-Evo) algorithms, can also be competitive and even sometimes outperform RNN-based controllers. One main difference between Reg-Evo and NEAT algorithms is that Reg-Evo’s model evolution method discards the oldest model in a population, in order to allow better diversity and exploration, while NEAT may discard models according to their performance or do not discard them at all, resulting in models that remain alive in the population for a long time. Another significant difference is that unlike NEAT which mutates both the architecture and weights in a randomized fashion, Reg-Evo only affects the architecture update method, allowing the user to define their own weight updating scheme (predominantly gradient descent). While the exact algorithm can be found in [37], in summary, Reg-Evo initializes with a population, or *queue* of n models $Q = \{m_1, \dots, m_n\}$ with corresponding scores (slightly abusing notation) $f(Q) = \{f(m_1), \dots, f(m_n)\}$ (or $f(Q, \theta_s)$ ’s instead in the efficient setting), and then proceeds to construct child models m' via mutating the model $m_{max} = \arg \max_{m \in Q} f(m)$ corresponding to the highest score. These child models are evaluated and appended to Q in a first-in, first-out (FIFO)-like manner, consequently removing the oldest model from Q , otherwise known as *tournament selection* [18].

Regardless of the controller used, the shared weights θ_s use a approximate gradient update:

$$\theta_s \leftarrow \theta_s + \eta_w \left(\frac{1}{n} \sum_{i=1}^n \nabla_{\theta_s} f(m_i, \theta_s) \right) \quad (2)$$

assuming the existence of such a gradient $\nabla_{\theta_s} f(m, \theta_s)$ that can be computed for any m . However, this can be fairly tricky to implement, as it requires operations on the model which still allow backpropagation regardless of potential disconnectivities in the graph.

With the advent of standardized NAS API such as PyGlove [35], as well as objective value databases such as NASBench [58], the search spaces of NAS problems have become highly similar to ones found in blackbox optimization. Such search spaces are usually constructed via combinations of primitives involving categorical and conditional parameters, such as ones found in hyperparameter optimization infrastructure [19]. Thus, a child model m can first simply be programmatically represented via Python dictionaries and strings to be sent over a distributed communication channel to a worker, and then materialized later by the worker into an actual neural network architecture.

2.2 Evolutionary Strategies/Augmented Random Search

Consider a fixed Markov Decision Process (MDP), or environment \mathcal{E} with state space $\mathcal{S} \subseteq \mathbb{R}^{|\mathcal{S}|}$ and action space $\mathcal{A} \subseteq \mathbb{R}^{|\mathcal{A}|}$ and an agent aiming to maximize its total expected/discounted reward obtained from interacting in \mathcal{E} . In deep reinforcement learning, the standard approach is to construct a neural network policy $\pi_{\theta}(s) = a$ which maps states $s \in \mathcal{S}$ to actions $a \in \mathcal{A}$, and is parameterized by θ , the neural network’s weights. The objective is to maximize the sum of rewards $\sum_{t=1}^T r_t$ obtained in the environment from a given trajectory of states and actions $(s_1, a_1, s_2, a_2, \dots, s_T, a_T)$.

ES [40]/ARS [30] interpret the sum of rewards as a blackbox objective $f(\theta) = \sum_{t=1}^T r_t$, and thus estimates the gradient of the Gaussian-smoothed objective $\tilde{f}_{\sigma}(\theta) = \mathbb{E}_{\mathbf{g} \sim \mathcal{N}(0, I)} [f(\theta + \sigma \mathbf{g})]$ to be used as an ascent update: $\theta' = \theta + \eta_w \nabla_{\theta} \tilde{f}_{\sigma}(\theta)$ for some step size η_w and precision parameter σ . Note that the gradient can be expressed as a finite difference:

$$\nabla_{\theta} \tilde{f}_{\sigma}(\theta) = \frac{1}{2\sigma} \mathbb{E}_{\mathbf{g} \sim \mathcal{N}(0, I)} [(f(\theta + \sigma \mathbf{g}) - f(\theta - \sigma \mathbf{g})) \mathbf{g}] \quad (3)$$

which can thus be estimated via sampling multiple $\mathbf{g}_1, \dots, \mathbf{g}_n$:

$$\nabla_{\theta} \tilde{f}_{\sigma}(\theta) = \frac{1}{\sigma n} \sum_{i=1}^n \frac{f(\theta + \sigma \mathbf{g}_i) - f(\theta - \sigma \mathbf{g}_i)}{2} \mathbf{g}_i \quad (4)$$

This algorithm is highly popularized in robotics applications [4, 17, 30, 46, 60] due to its ability to use *deterministic* and sometimes *linear* policies, allowing for stable control and fast inference, as opposed to necessarily using stochastic policies employed by policy gradient algorithms, or complex and relatively slow argmax procedures for Q-learning in continuous control.

Furthermore, this algorithm can run on CPUs via a distributed pipeline, and does not require differentiable components as it does not use exact backpropagation, a property previously exploited to allow sorting mechanisms [52] and argmax operations [44]. In our particular setting, this flexibility allows fast modifications between different types of combinatorial policies, as we will see in the experimental section.

A more advanced variant of this approach is CMA-ES [23] which consists of sampling $\mathbf{g} \sim \mathcal{N}(0, \mathbf{C})$ where \mathbf{C} is a covariance matrix. However, despite its power, the computation of the full covariance matrix is non-trivial, and because of this, CMA-ES is rarely applied to problems in high-dimensional space [33] where ES is already satisfactory. Nonetheless, since CMA-ES is still based on a blackbox aggregator-worker framework, it is clear that it may also be used in our ES-ENAS approach, which we describe below.

3 ES-ENAS METHOD

3.1 Weight and Controller Updates

The optimization problem we are interested in is $\max_{m, \theta} f(m, \theta)$, which represents the sum of rewards over the environment by using a policy whose architecture is m , and weights are θ .

Note that if m is sampled from an controller p_{ϕ} where ϕ expresses the controller state (e.g. RNN parameters for Policy Gradient or model population for Regularized Evolution) of the controller, in addition to the usual Gaussian smoothing of θ , then the smoothed

objective becomes:

$$\tilde{f}_\sigma(\phi, \theta) = \mathbb{E}_{m \sim p_\phi, \mathbf{g} \sim \mathcal{N}(0, \mathbf{I})} [f(m, \theta + \sigma \mathbf{g})] \quad (5)$$

3.1.1 Updating the Weights. The gradient with respect to θ becomes:

$$\nabla_\theta \tilde{f}_\sigma(\phi, \theta) = \frac{1}{2\sigma} \mathbb{E}_{m \sim p_\phi, \mathbf{g} \sim \mathcal{N}(0, \mathbf{I})} [(f(m, \theta + \sigma \mathbf{g}) - f(m, \theta - \sigma \mathbf{g})) \mathbf{g}] \quad (6)$$

Note that by linearity, we may move the expectation $\mathbb{E}_{m \sim p_\phi}$ inside into the two terms $f(m, \theta + \sigma \mathbf{g})$ and $f(m, \theta - \sigma \mathbf{g})$, which implies that the gradient expression can be estimated with averaging singleton samples of the form:

$$\frac{1}{2\sigma} (f(m^+, \theta + \sigma \mathbf{g}) - f(m^-, \theta - \sigma \mathbf{g})) \mathbf{g} \quad (7)$$

where m^+ , m^- are i.i.d. samples from p_ϕ , and \mathbf{g} from $\mathcal{N}(0, \mathbf{I})$.

3.1.2 Updating the Controller. If the controller p_ϕ is an RNN parameterized by ϕ , then in order to optimize ϕ , we see that this corresponds to sending the reward $R(m) = \mathbb{E}_{\mathbf{g} \sim \mathcal{N}(0, \mathbf{I})} [f(m, \theta + \sigma \mathbf{g})]$ given a model m in order to produce the policy gradient sample $\nabla_\phi R(m) \log p_\phi(m)$. However, practically speaking, this corresponds to actually sending in a stochastic reward $f(m, \theta + \sigma \mathbf{g})$ from a sampled \mathbf{g} . Similarly, if the controller p_ϕ is Reg-Evo, then we may simply pass in $f(m, \theta + \sigma \mathbf{g})$ as the model objective into the population and run the algorithm as-is.

This mechanism shows that updates to the controller p and updates to the weights θ both rely on the samples $f(m, \theta + \sigma \mathbf{g})$. The number of workers n , now serves the two purposes: reducing the sample complexity of the controller p , as well as the variance of the estimated ES gradient $\nabla_\theta \tilde{f}_\sigma$. We show the conceptual simplicity of combining the two updates in Algorithm 1.

Algorithm 1: ES-ENAS Algorithm, with the few additional modifications to allow ENAS shown in blue.

Data: Initial weights θ_s , weight step size η_w , precision parameter σ , number of perturbations n , controller

p_ϕ .

while not done do

 Sample i.i.d. vectors $\mathbf{g}_1, \dots, \mathbf{g}_n \sim \mathcal{N}(0, \mathbf{I})$;

foreach \mathbf{g}_i **do**

 Sample $m_i^+, m_i^- \sim p_\phi$

$v_i^+ \leftarrow f(m_i^+, \theta_s + \sigma \mathbf{g}_i)$

$v_i^- \leftarrow f(m_i^-, \theta_s - \sigma \mathbf{g}_i)$

$v_i \leftarrow \frac{1}{2}(v_i^+ - v_i^-)$

$p_\phi \leftarrow \{(m_i^+, v_i^+), (m_i^-, v_i^-)\}$

end

 Update weights $\theta_s \leftarrow \theta_s + \eta_w \frac{1}{\sigma n} \sum_{i=1}^n v_i \mathbf{g}_i$

 Update controller p_ϕ

end

In the distributed setting of the aggregator-worker case, the model m can be serialized into a string, contained in the original message containing a perturbation $\theta + \sigma \mathbf{g}$ from the aggregator to one of the workers. The worker then materializes the model and uses forward-passes to interact in the environment \mathcal{E} . Although the controller needs to output hundreds of model suggestions, it

can be parallelized to run quickly by multithreading (for Reg-Evo) or by simply using a GPU (for policy gradient).

3.2 Extensions

We note a few extensions and modifications of this work as well:

- A similar setup can be potentially made when using distributed policy gradient or Q-learning algorithms, where the **aggregator also receives state-action pairs from various sampled models**. Combining these RL algorithms with NAS may be of interest for exploration in later works. However, we believe that ES is more naturally suited for the efficient setup, as it is relatively simple both conceptually and in terms of implementation, requiring only a network’s forward pass rather than backward pass, which reduces complexity in a weight sharing pipeline. Furthermore, ES usually uses many more workers (on the order of 10^2) than the distributed variants of the other methods (on the order of 10^0 to 10^1 of workers) which can be important for the controller’s performance, as we will show in Subsection 5.5.
- The **controller p_ϕ ’s objective can also be defined differently from the weights θ_s ’s objective**. This is already subtly the case in supervised learning, where the controller’s objective is the *nondifferentiable validation accuracy* of the model, while the model weights are explicitly optimizing against the *differentiable cross-entropy training loss* of the model. More significant differences between the controller objective and weight objective involve cases such as efficiency and runtime of the network, which have led to work in EfficientNets [51]. We show this can also be applied for the RL setting in Subsection 5.6.
- Lastly, the controller does not need to be use policy gradients or Reg-Evo, although they are the most popular. Other algorithms may also be used, as the controller simply needs to collect objectives and suggest new models. However, both controllers are readily packaged in PyGlove along with search space primitives, we opt to use these methods.

4 APPLICATIONS

While the mentioned ES-ENAS algorithm is a general purpose algorithm which allows a multitude of potential applications and modifications, we provide below example applications that are relevant with literature in mobile robotics, which can leverage combinatorial search spaces and also use our ES-ENAS algorithm. Due to the **very extensive** background work regarding pruning and compression techniques as we discuss in the next subsections, we thus emphasize to the reader that we will not claim to achieve state of the art for compression on RL policies. We rather instead, demonstrate how our method can apply diverse NAS techniques from SL on a reasonably challenging search space in RL, especially since unlike SL [58], there are no standardized NAS benchmarks in RL. However, as we will discuss in Subsection 5.1, our RL search space is similar or even larger in size compared to NASBench [58]. Whereas some of the background works’ algorithms can only be applied to specific problems, ES-ENAS’s versatility lies in its applicability to general search spaces.

One application of network compression is in mobile robotics [15], where computational and storage resources are very limited (especially without an on-board GPU), and there is a need for fast inference times to manage high-frequency reaction speeds (on the order of miliseconds), as well as a need for low memory usage. Furthermore, there has been recent interest in simple policies for continuous control. In particular, [30] demonstrated that linear policies are often sufficient for the benchmark MuJoCo locomotion tasks, while [8] found smaller policies could work for vision-based tasks by separating feature extraction and control. Finally, recent work found that small, sparse sub-networks can perform better than larger over-parameterized ones [13], inspiring applications in RL [59].

Two recent papers come to mind: [5] and [16]. In the former one, policies based on Toeplitz matrices were shown to match their unstructured counterparts accuracy-wise, while leading to the substantial reduction of the number of parameters from thousands [40] to hundreds [5]. Instead of quadratic (in sizes of hidden layers), those policies use only linear number of parameters. The Toeplitz structure can be thought of as a parameter sharing mechanism, where edge weights along each diagonal of the matrix are the same (see: Fig. 3).

The latter paper [16] proposes an extremal approach, where weights are chosen randomly instead of being learned, but the topologies of connections are trained and thus are ultimately strongly biased towards RL tasks under consideration. It was shown in [16] that such Weight Agnostic Neural Networks (WANNs) can encode effective policies for several nontrivial RL problems. WANNs replace conceptually simple feedforward networks with general graph topologies using NEAT [48], providing topological operators to build the network. However, aligned with the principles of NEAT, WANNs focus heavily on requiring a single (random) weight and cannot be used on tasks with rich sets of weights which need to be trained with gradient descent. Furthermore, WANNs may require relatively complicated connections to be memorized, which may not be suitable for mobile robotics. Nonetheless, we are inspired by such a technique and thus allow searching for different nonlinearities across the nodes of our neural network.

The above two examples lead us to a middle ground set of methods, which can be more natural and easier to implement with an emphasis on reducing complexity and parameter count from a broad range of aspects: **sparsification** and **weight sharing**, in addition to **nonlinearity searching**. In the first two settings, the topology is still a feedforward neural network, but in the former case, we simply determine whether each edge in the network to mask or not, while in the latter case, the weights are partitioned into groups, with each group using the same scalar weight value.

4.1 Sparsification

There is vast literature on compact encodings of NN architectures, with some of the most popular and efficient techniques regarding network sparsification. The sparsity can be often achieved by *pruning* already trained networks. These methods have been around since the 1980s, dating back to Rumelhart [2, 32, 39], followed shortly by Optimal Brain Damage [9], which used second order

gradient information to remove connections. Since then, a variety of schemes have been proposed, with regularization [29] and magnitude-based weight pruning methods [22, 34, 42] increasingly popular. The impact of *dropout* [47] has added an additional perspective, with new works focusing on attempts to learn sparse networks [20]. Another recent work introduced the Lottery Ticket Hypothesis [13], which captivated the community by showing that there exist equivalently sparse networks which can be trained from scratch to achieve competitive results. Indeed, [26] do achieve state-of-the-art results on various supervised feedforward and recurrent models. Interestingly, these works consistently report similar levels of compression, often managing to match the performance of original networks with up to 90% fewer parameters. Those methods are however designed for constructing classification networks rather than those encoding RL policies. We ultimately confirm these findings in the RL setting by showing that good rewards can be obtained up to a high level of pruning.

4.2 Weight Sharing and Quantization

Weight sharing mechanisms can be viewed from the quantization point of view, where pre-trained weights are quantized, thus effectively partitioned. Examples include [21], who achieve 49x compression for networks applied for vision using both pruning and weight sharing (by quantization) followed by Huffman coding, [3], which compresses networks via randomized weight sharing, and [11], which uses hashing mechanisms to achieve competitive results against EfficientNets [51] in image classification. More relevantly, [5] hardcodes RL policies using specific *Toeplitz* matrices and found that such weight sharing patterns work well in control. However such partitions are not learned which is a main topic of this paper. Even more importantly, in RL applications, where policies are often very sensitive to parameters' weights [24], centroid-based quantization may be too crude to preserve accuracy.

5 EXPERIMENTAL RESULTS

The experimental section is organized as follows:

- In Subsections 5.1, 5.2, and 5.3, we describe the search space definitions, baseline methods, and environments used, respectively.
- In Subsections 5.4, 5.5, and 5.6, we discuss the ablation results and extra modifications of the ES-ENAS method via plots. These results include respectively: comparisons across different controllers, sample complexity with respect to using varying numbers of workers, as well as multiobjective optimization.
- In Subsection 5.8, we present exhaustive tabular results displaying the final rewards across different methods.

We provide more experimental results in the Appendix.

5.1 Search Space Definitions

In order to allow combinatorial flexibility, our neural network consists of vertices/values $V = \{v_1, \dots, v_k\}$, where the initial block of $|\mathcal{S}|$ values $\{v_1, \dots, v_{|\mathcal{S}|}\}$ corresponds to the environment state, and the last block of $|\mathcal{A}|$ values $\{v_{k-|\mathcal{A}|+1}, \dots, v_k\}$ corresponds to the action output values. Directed edges $E \subseteq E_{max} = \{e_{i,j} = (i, j) \mid |\mathcal{S}| < i < j \leq k\}$ are constructed with corresponding weights

$W = \{w_{i,j} \mid (i,j) \in E\}$, and nonlinearities $F = \{f_{|S|+1}, \dots, f_k\}$ for the non-state vertices. Thus a forward propagation consists of for-looping in order $j \in \{|S|+1, \dots, k\}$ and computing output values $v_j = f_j \left(\sum_{(i,j) \in E} v_i w_{i,j} \right)$.

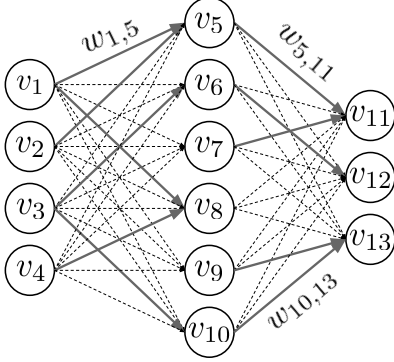


Figure 2: Example of our neural network setup with selected edges and corresponding weight labels, when $|S| = 4$ and $|\mathcal{A}| = 3$, with a hidden layer of size 6. Solid edges are those learned by the algorithm.

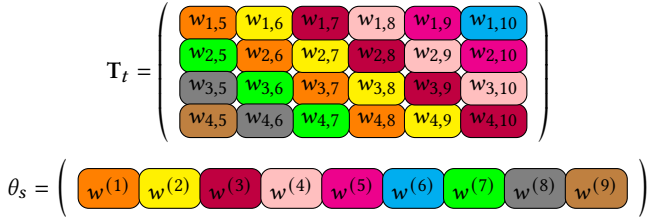


Figure 3: Example of weight sharing mechanism using a Toeplitz pattern [5], for the first layer in Fig. 2. Entries in each of the diagonals are colored the same, thus sharing the same weight value. The trainable weights $\theta_s = (w^{(1)}, \dots, w^{(9)})$ are denoted at the very bottom in the vectorized form. As we see, a weight matrix with 24 entries is effectively encoded by a 9-dimensional vector.

Thus, for our **edge pruning** method, we group all possible edges (i,j) into a set in the neural network, and select a fixed number of edges from this set. We can also further search across potentially different nonlinearities, e.g. $f_i \in \{\tanh, \text{sigmoid}, \sin, \dots\}$. For our **weight sharing** method, we assign to each edge (i,j) one color of many colors $c \in C = \{1, \dots, |C|\}$, denoting the partition group the edge is assigned to, which defines the value $w_{i,j} \leftarrow w^{(c)}$. This is shown pictorially in Figs. 2 and 3.

Note that in both cases, the size $|\mathcal{M}|$ of the search space is exponentially large; for edge-pruning this is $\binom{|E_{max}|}{|E|}$ or $2^{|E_{max}|}$ when using a fixed or variable size $|E|$ respectively, and for weight sharing, this is $|C|^{|E|}$. These sizes are calculated to be greater than 10^{68} (comparable to 10^{49} , the size of NASBench’s search space [58]) when using our specific hyperparameters, whose details can be found in Appendix C.2. Thus, a purely random search will clearly be unable to exhaust the entire search space, and will also likely have difficulty attaining high rewards, which we confirm as a sanity check in Subsection 5.4.

In terms of actual code, combinatorial search spaces can be defined in terms of default search space *primitives* in PyGlove [35], with the most prominent being the "pyglove.oneof" and "pyglove.manyof" operations, which respectively choose one item, or a combination of multiple objects from a container. These primitives may be combined in a nested structure via "pyglove.List" or "pyglove.Dict". Thus, for edge pruning, we may simply define the search space as `pyglove.manyof($E_{max}, |E|$)` as well as concatenating primitives `pyglove.oneof($e_{i,j}, C$)` over all edges $e_{i,j} \in E_{max}$ for the edge pruning method. The search space may then be sent to a pre-implemented controller (such is the case for Reg-Evo, Policy Gradient, and pure random search), which proposes instances from the space. Thus, due to the simplicity of the PyGlove API, we see that appending a NAS pipeline into preexisting ES code is quite clean and straightforward.

5.2 Baseline Definitions

In our experiments, we also include specific baselines, including a DARTS-like [28] softmax *masking* method [26], where a trainable boolean matrix mask is drawn from a multinomial distribution, and element-wise multiplied with the weights before a forward pass. We also include the results from using Toeplitz and Circulant (particular class of Toeplitz) matrices as weights from referenced works [5]. Specific details can be found in Appendices B.1 and C.2.

5.3 Environments

We perform experiments on the following OpenAI Gym tasks: Swimmer, Reacher, Hopper, HalfCheetah, Walker2d, Pusher, Striker, Thrower, and Ant. These environments for continuous control are commonly used for demonstrating the validity of RL methods, including popular algorithms such as PPO [41], DDPG [27] and the original ES/ARS [30, 40]. For all environments which are simulated in the physics engine Mujoco [53], the state consists of a 1-D vector containing data such as the joint/arm positions and velocities of an agent, while the action consists of applying force via its limbs. The reward is a combination of forward movement penalized by energy loss from applying actions, which encourages efficient movement.

5.4 Controller Comparisons

We first compare between the random, Policy Gradient (PG), and Reg-Evo controllers in Fig. 4 on the edge pruning task. While we clearly see that the random controller usually does poorly, we find that the PG and Reg-Evo controllers both perform well on various tasks, with one outperforming the other depending on the type of task. We further find that in most cases, the Reg-Evo controller converges much faster, although the PG controller may sometimes end up with a higher asymptotic performance. Intriguingly, PG produces generally higher variance between runs as well. This is intriguing, as there is no clear winner between PG and Reg-Evo, unlike in supervised learning (SL) where it is usually clear that the now widely adopted Reg-Evo outperforms PG [37].

On the topic of random search, we find our results somewhat consistent compared to NAS in supervised learning (SL) - random search in SL sampled from a reasonable search space can produce ≥ 80 -90 % accuracy [36, 37] with the most gains from NAS ultimately be at the tail end; e.g. at the 95% accuracies, which is also shown to

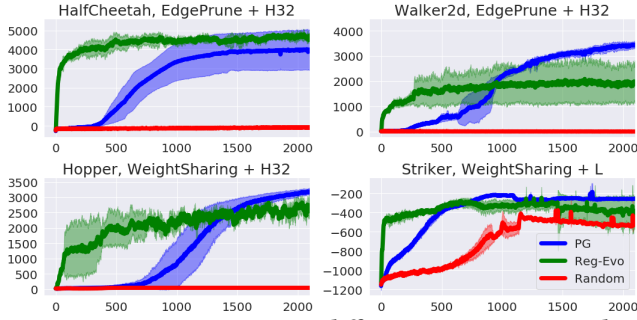


Figure 4: Comparisons across different environments when using different controllers, on the edge pruning and weight sharing tasks, when using a linear layer (L) or hidden layer of size 32 (H32).

a lesser degree for easier RL environments such as Striker (shown in Fig. 4) and Reacher (shown in Appendices B.2, B.3), although for the majority of RL environments, random search is unable to train at all.

5.5 Controller Sample Complexity

We further investigate the effect of the number of objective values per batch on the controller by randomly selecting only a subset of the objectives $f(m, \theta)$ for the controller p_ϕ to use, but maintain the original number of workers for updating θ_s via ES to maintain weight estimation quality to prevent confounding results. We found that this sample reduction can reduce the performance of both controllers for various tasks, especially the PG controller. Thus, we find the use of the already present ES workers highly crucial for the controller’s quality of architecture search in this setting.

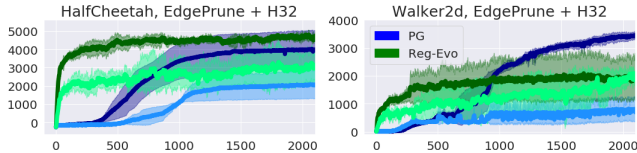


Figure 5: Regular ES-ENAS experiments with 150 full controller objective value usage plotted in darker colors. Experiments with lower controller sample usage (10 random samples, similar to the number of simultaneously training models in [50]) plotted in corresponding lighter colors.

5.6 Multiobjective Case

[50, 51] introduce the powerful notion of *Multiobjective Optimization*, where the controller may optimize multiple objectives towards a Pareto optimal solution [10]. Similar to [50]’s approach, we can modify the controller’s objective to be a hybrid combination $f(\theta, m) \left(\frac{|E_m|}{|E_T|} \right)^\omega$ of both the total reward $f(\theta)$ and the compression ratio $\frac{|E_m|}{|E_T|}$ where $|E_m|$ is the number of edges in model m and $|E_T|$ is a target number, and allow the controller to decide the number of edges on a Pareto optimal solution rather strictly use a human specified hyperparameter. We thus express our search space as boolean mask mappings $(i, j) \rightarrow \{0, 1\}$ over all possible edges. For proof-of-concept, we follow the basic specifications in [50] and set

$\omega = -1$ if $\frac{|E_m|}{|E_T|} > 1$, while $\omega = 0$ otherwise, which strongly penalizes the controller if it proposes a model m whose edge number $|E_m|$ breaks the threshold $|E_T|$. However, as noted in [50], ω can be more finely tuned to allow $|E_T|$ to be a softer constraint and the hybrid objective to be smoother, if the user empirically knows the tradeoff between number of edges and reward.

In Fig. 6, we see that the controller eventually reduces the number of edges below the target threshold set at $|E_T| = 64$, while still maintaining competitive training reward, demonstrating the versatility of the multiobjective approach in the RL setting.

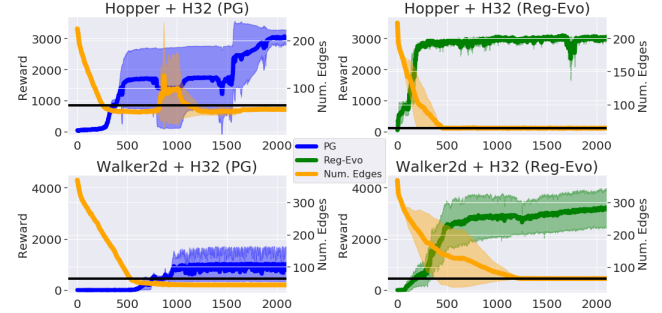


Figure 6: Environment reward plotted alongside the average number of edges used for proposed models. Black horizontal line corresponds to the target $|E_T| = 64$.

5.7 Visualizing Convergence

In order to confirm convergence results of ES-ENAS, we also graphically plot aggregate statistics over the controller samples. In order to best depict this effect and reduce the visual complexity of observing many edges, we select the smallest environment possible, Swimmer, which has dimensions (8,2). Coincidentally, it is a common phenomenon that the Swimmer environment is biased towards *linear* policies, where a linear policy can achieve an award of around ≈ 360 , whereas hidden layer policies can usually only achieve ≈ 100 [30, 41], suggesting that fewer edges may actually help performance. Thus, we also define the edge pruning search space to be a subset of a linear policy, which avoids needing to deal with permutation equivalencies if using a hidden layer, further reducing visual complexity. We also select our edge pruning search space to be boolean to allow the controller full control over selecting every edge rather than a fixed number of edges which increases the size ($2^{8 \times 2} = 2^{16}$) of the search space, but nevertheless remarkably observe that *for all 3 independently seeded runs*, both PG controller converges toward a specific "local maximum" architecture, demonstrated in Fig. 7. We found this to be true for Reg-Evo as well, although its final architecture was different than PG’s, suggesting that there may be a few natural architectures optimal to the environment depending on the controller algorithm. We present PG’s final architecture in Appendix A as well as other plots, including results from weight sharing.

5.8 Full Results

The full set of numerical results over all of the mentioned methods can be found in Appendix B, which includes the weight sharing (Appendix B.2), edge pruning (Appendix B.3), as well as plots for baseline methods (Fig. 10).

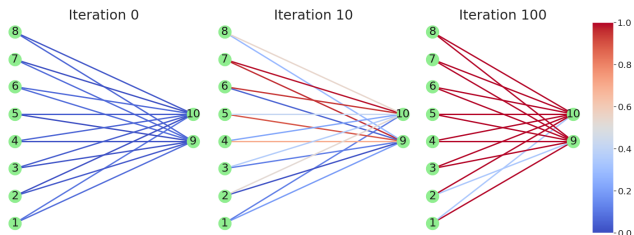


Figure 7: Edge pruning convergence over time, with samples aggregated over 3 seeds from PG runs on Swimmer. Each edge is colored according to a spectrum, with its color value equal to $2|p - \frac{1}{2}|$ where p is the edge frequency. We see that initially, each edge has uniform ($p = \frac{1}{2}$) probability of being selected, but as the controller trains, the samples converge toward a single pruning.

However, we present the some of the more notable results in Table 1. Intriguingly, we found that appending the extra nonlinearity selection into the edge-pruning search space improved performance across HalfCheetah and Swimmer, but not across all environments (see Appendix B.4). However, lack of total improvement is consistent with the results found with WANNs [16], which also showed that trained WANNs’ performances matched with vanilla policies. From these two observations, we hypothesize that perhaps nonlinearity choice for simple MLP policies trained via ES are not quite so important to performance as other components, but more ablation studies must be conducted. Furthermore, for weight sharing policies, we see that hidden layer policies near-universally outperform linear policies, even when using the same number of distinct weights.

Env.	Dim.	(PG, Reg-Evo) Reward	Method
HalfCheetah	(17,6)	(2958, 3477) → (4258, 4894)	Weight Sharing (L → H)
Hopper	(11,3)	(2097, 1650) → (3288, 2834)	Weight Sharing (L → H)
HalfCheetah	(17,6)	(2372, 4016) → (3028, 5436)	Edge Pruning (H) → (+ Nonlinearity Search)
Swimmer	(8,2)	(105, 343) → (247, 359)	Edge Pruning (H) → (+ Nonlinearity Search)

Table 1: Rewards for selected environments and methods, each result averaged over 3 seeds. Arrow denotes modification or addition (+).

In Table 2 we directly compare our methods with the masking approach discussed in Subsection 5.2 and (in more detail in Appendix B.1), as well as other structured policies (Toeplitz from [5] and Circulant) and the unstructured baseline. In all cases we use the same hyper-parameters, and train until convergence for three random seeds. For masking, we report the best achieved reward with $> 90\%$ of the network pruned, making the final policy comparable in size to the weight sharing and edge-pruning networks.

For each class of policies, we compare the number of weight parameters used (“# of weight-params” field), since the compactification mechanism does not operate on bias vectors. We also record compression with respect to unstructured networks in terms of the total number of parameters including biases (“# compression” field).

This number determines the reduction of sampling complexity with respect to unstructured networks (which is a bottleneck of ES training), since generally for ES, the number of blackbox function $f(\theta)$ queries needed to optimize f is proportional to the length of θ , which is equal to the total number of weights and biases of a policy network π_θ [1, 25, 49].

Env.	Arch.	Reward	# weights	compression	# bits
Striker	Weight Sharing	-247	23	95%	8198
	Edge Pruning	-130	64	93%	3072
	Masked	-967	25	95%	8262
	Toeplitz	-129	110	88%	4832
	Circulant	-120	82	90%	3936
	Unstructured	-117	1230	0%	40672
HalfCheetah	Weight Sharing	4894	17	94%	6571
	Edge Pruning	4016	64	98%	3072
	Masked	4806	40	92%	8250
	Toeplitz	2525	103	85%	4608
	Circulant	1728	82	88%	3936
	Unstructured	3614	943	0%	31488
Hopper	Weight Sharing	3220	11	92%	3960
	Edge Pruning	3349	64	84%	3072
	Masked	2196	17	91%	4726
	Toeplitz	2749	94	78%	4320
	Circulant	2680	82	80%	3936
	Unstructured	2691	574	0%	19680
Walker2d	Weight Sharing	2026	17	94%	6571
	Edge Pruning	3813	64	90%	3072
	Masked	1781	19	94%	6635
	Toeplitz	1	103	85%	4608
	Circulant	3	82	88%	3936
	Unstructured	2230	943	0%	31488

Table 2: Comparison of the best policies from six distinct classes of RL networks: Weight Sharing (ours), Edge Pruning (ours), Masked, Toeplitz, Circulant, and Unstructured networks trained with standard ES algorithm [40]. All results are for feedforward nets with one hidden layer. Top two performing networks for each environment are in bold.

Finally, for a working policy we report total number of bits required to encode it assuming that real values are stored in the float format. Note that for weight sharing and masking networks, this includes bits required to encode a dictionary representing the partitioning.

6 CONCLUSION & FUTURE WORK

We presented a scalable and flexible algorithm, ES-ENAS, for performing efficient neural architecture search for reinforcement learning policies by combining Evolutionary Strategies with a NAS controller. ES-ENAS is compatible the latest frameworks (blackbox optimization [58] and decoupling via PyGlove [35]), as well as the latest techniques for NAS (multiobjective optimization [50, 51] and regularized evolution [37]).

While we have shown an example utility of ES-ENAS on learning structured neural network architectures for RL policies via edge pruning and weight sharing, we believe that this work can be the start of a new line of thinking for NAS methods applied to RL. One highly impactful application may be designing convolutional cells for vision-based RL policies to improve generalization [6, 7, 45], similar to the search spaces found in standard SL applications [36, 51, 58]. One may use similar search spaces to design EfficientNet variants for vision-based RL as well, an extension of the multiobjective experiments found in this paper for dense layers. We hope that applying NAS techniques in RL may ultimately automate architecture design for policies, as well as change perspectives on designing human-made policies.

7 ACKNOWLEDGEMENTS

The authors would like to thank David Ha, Yingjie Miao, Aleksandra Faust, Sagi Perel, Daniel Golovin, John D. Co-Reyes, and Vikas Sindhwani for valuable discussions.

REFERENCES

- [1] Alekh Agarwal, Dean P. Foster, Daniel J. Hsu, Sham M. Kakade, and Alexander Rakhlin. 2011. Stochastic convex optimization with bandit feedback. In *Advances in Neural Information Processing Systems 24: 25th Annual Conference on Neural Information Processing Systems 2011. Proceedings of a meeting held 12-14 December 2011, Granada, Spain*. 1035–1043. <http://papers.nips.cc/paper/4475-stochastic-convex-optimization-with-bandit-feedback>
- [2] Yves Chauvin. 1989. A Back-propagation Algorithm with Optimal Use of Hidden Units. In *Advances in Neural Information Processing Systems 1*, David S. Touretzky (Ed.). Morgan Kaufmann Publishers Inc., San Francisco, CA, USA, 519–526.
- [3] Wenlin Chen, James Wilson, Stephen Tyree, Kilian Weinberger, and Yixin Chen. 2015. Compressing Neural Networks with the Hashing Trick. In *International Conference on Machine Learning*. 2285–2294.
- [4] Krzysztof Choromanski, Aldo Pacchiano, Jack Parker-Holder, Yunhao Tang, Deepali Jain, Yuxiang Yang, Atil Iscen, Jasmine Hsu, and Vikas Sindhwani. 2019. Provably Robust Blackbox Optimization for Reinforcement Learning. In *3rd Annual Conference on Robot Learning, CoRL 2019, Osaka, Japan, October 30 - November 1, 2019, Proceedings*. 683–696. <http://proceedings.mlr.press/v100/choromanski20a.html>
- [5] Krzysztof Choromanski, Mark Rowland, Vikas Sindhwani, Richard E. Turner, and Adrian Weller. 2018. Structured Evolution with Compact Architectures for Scalable Policy Optimization. In *Proceedings of the 35th International Conference on Machine Learning, ICML 2018, Stockholm, Sweden, July 10-15, 2018*. 969–977.
- [6] Karl Cobbe, Christopher Hesse, Jacob Hilton, and John Schulman. 2020. Leveraging Procedural Generation to Benchmark Reinforcement Learning. In *Proceedings of the 37th International Conference on Machine Learning, ICML 2020, 13-18 July 2020, Virtual Event*. 2048–2056. <http://proceedings.mlr.press/v119/cobbe20a.html>
- [7] Karl Cobbe, Oleg Klimov, Christopher Hesse, Taehoon Kim, and John Schulman. 2019. Quantifying Generalization in Reinforcement Learning. In *Proceedings of the 36th International Conference on Machine Learning, ICML 2019, 9-15 June 2019, Long Beach, California, USA*. 1282–1289. <http://proceedings.mlr.press/v97/cobbe19a.html>
- [8] Giuseppe Cuccu, Julian Togelius, and Philippe Cudré-Mauroux. 2019. Playing Atari with Six Neurons. In *Proceedings of the 18th International Conference on Autonomous Agents and Multi-Agent Systems (AAMAS '19)*. Richland, SC, 9.
- [9] Yann Le Cun, John S. Denker, and Sara A. Solla. 1990. Optimal Brain Damage. In *Advances in Neural Information Processing Systems 2*, David S. Touretzky (Ed.). Morgan Kaufmann Publishers Inc., San Francisco, CA, USA, 8.
- [10] Kalyanmoy Deb. 2005. *Multi-Objective Optimization*. Springer US. 273–316 pages. https://doi.org/10.1007/0-387-28356-0_10
- [11] Elad Eban, Yair Movshovitz-Attias, Hao Wu, Mark Sandler, Andrew Poon, Yerlan Idelbayev, and Miguel Á. Carreira-Perpiñán. 2020. Structured Multi-Hashing for Model Compression. In *2020 IEEE/CVF Conference on Computer Vision and Pattern Recognition, CVPR 2020, Seattle, WA, USA, June 13-19, 2020*. 11900–11909. <https://doi.org/10.1109/CVPR42600.2020.01192>
- [12] Thomas Elsken, Jan Hendrik Metzen, and Frank Hutter. 2019. Neural Architecture Search: A Survey. *Journal of Machine Learning Research* 20 (2019), 55:1–55:21.
- [13] Jonathan Frankle and Michael Carbin. 2019. The Lottery Ticket Hypothesis: Finding Sparse, Trainable Neural Networks. In *International Conference on Learning Representations*.
- [14] Peter I. Frazier. 2018. A Tutorial on Bayesian Optimization. *CoRR* abs/1807.02811 (2018). [arXiv:1807.02811](https://arxiv.org/abs/1807.02811) <http://arxiv.org/abs/1807.02811>
- [15] Douglas W. Gage (Ed.). 2002. *Mobile Robots XVII, Philadelphia, PA, USA, October 25, 2004*. SPIE Proceedings, Vol. 5609. SPIE. <http://proceedings.spiedigitallibrary.org/volume.aspx?volume=5609>
- [16] Adam Gaier and David Ha. 2019. Weight Agnostic Neural Networks. In *Advances in Neural Information Processing Systems 32: Annual Conference on Neural Information Processing Systems 2019, NeurIPS 2019, December 8-14, 2019, Vancouver, BC, Canada*. 5365–5379. <http://papers.nips.cc/paper/8777-weight-agnostic-neural-networks>
- [17] Wenbo Gao, Laura Graesser, Krzysztof Choromanski, Xingyou Song, Nevena Lazic, Pannag Sanketi, Vikas Sindhwani, and Navdeep Jaitly. 2020. Robotic Table Tennis with Model-Free Reinforcement Learning. (2020). <https://arxiv.org/abs/2003.14398>
- [18] David E. Goldberg and Kalyanmoy Deb. 1990. A Comparative Analysis of Selection Schemes Used in Genetic Algorithms. In *Proceedings of the First Workshop on Foundations of Genetic Algorithms. Bloomington Campus, Indiana, USA, July 15-18 1990*. 69–93. <https://doi.org/10.1016/b978-0-08-050684-5.50008-2>
- [19] Daniel Golovin, Benjamin Solnik, Subhodeep Moitra, Greg Kochanski, John Karro, and D. Sculley. 2017. Google Vizier: A Service for Black-Box Optimization. In *Proceedings of the 23rd ACM SIGKDD International Conference on Knowledge Discovery and Data Mining, Halifax, NS, Canada, August 13 - 17, 2017*. 1487–1495. <https://doi.org/10.1145/3097983.3098043>
- [20] Aidan N. Gomez, Ivan Zhang, Kevin Swersky, Yarin Gal, and Geoffrey E. Hinton. 2019. Learning Sparse Networks Using Targeted Dropout. *ArXiv* abs/1905.13678 (2019).
- [21] Song Han, Huizi Mao, and William J. Dally. 2016. Deep Compression: Compressing Deep Neural Network with Pruning, Trained Quantization and Huffman Coding. In *International Conference on Learning Representations*.
- [22] Song Han, Jeff Pool, John Tran, and William Dally. 2015. Learning both Weights and Connections for Efficient Neural Network. In *Advances in Neural Information Processing Systems 28*, C. Cortes, N. D. Lawrence, D. D. Lee, M. Sugiyama, and R. Garnett (Eds.). Curran Associates, Inc., 1135–1143.
- [23] Nikolaus Hansen, Sibylle D. Müller, and Petros Koumoutsakos. 2003. Reducing the Time Complexity of the Derandomized Evolution Strategy with Covariance Matrix Adaptation (CMA-ES). *Evol. Comput.* 11, 1 (March 2003), 1–18.
- [24] Atıl Iscen, Ken Caluwaerts, Jie Tan, Tingnan Zhang, Erwin Coumans, Vikas Sindhwani, and Vincent Vanhoucke. 2018. Policies Modulating Trajectory Generators. In *2nd Annual Conference on Robot Learning, CoRL 2018, Zürich, Switzerland, 29-31 October 2018, Proceedings*. 916–926.
- [25] Kevin G. Jamieson, Robert D. Nowak, and Benjamin Recht. 2012. Query Complexity of Derivative-Free Optimization. In *Advances in Neural Information Processing Systems 25: 26th Annual Conference on Neural Information Processing Systems 2012. Proceedings of a meeting held December 3-6, 2012, Lake Tahoe, Nevada, United States*. 2681–2689. <http://papers.nips.cc/paper/4509-query-complexity-of-derivative-free-optimization>
- [26] Karel Lenc, Erich Elsen, Tom Schaul, and Karen Simonyan. 2019. Non-Differentiable Supervised Learning with Evolution Strategies and Hybrid Methods. *arXiv* abs/1906.03139 (2019).
- [27] Timothy P. Lillicrap, Jonathan J. Hunt, Alexander Pritzel, Nicolas Heess, Tom Erez, Yuval Tassa, David Silver, and Daan Wierstra. 2016. Continuous control with deep reinforcement learning. In *4th International Conference on Learning Representations, ICLR 2016, San Juan, Puerto Rico, May 2-4, 2016, Conference Track Proceedings*. <http://arxiv.org/abs/1509.02971>
- [28] Hanxiao Liu, Karen Simonyan, and Yiming Yang. 2019. DARTS: Differentiable Architecture Search. In *7th International Conference on Learning Representations, ICLR 2019, New Orleans, LA, USA, May 6-9, 2019*. <https://openreview.net/forum?id=S1eYHoC5FX>
- [29] Christos Louizos, Max Welling, and Diederik P. Kingma. 2018. Learning Sparse Neural Networks through L0 Regularization. In *International Conference on Learning Representations*.
- [30] Horia Mania, Aurelia Guy, and Benjamin Recht. 2018. Simple Random Search of Static Linear Policies is Competitive for Reinforcement Learning. In *Advances in Neural Information Processing Systems*. 1800–1809.
- [31] Horia Mania, Aurelia Guy, and Benjamin Recht. 2018. Simple random search provides a competitive approach to reinforcement learning. *CoRR* abs/1803.07055 (2018). [arXiv:1803.07055](https://arxiv.org/abs/1803.07055)
- [32] Michael C. Mozer and Paul Smolensky. 1989. Skeletonization: A Technique for Trimming the Fat from a Network via Relevance Assessment. In *Advances in Neural Information Processing Systems 1*, David S. Touretzky (Ed.). Morgan Kaufmann Publishers Inc., San Francisco, CA, USA, 107–115.
- [33] Nils Müller and Tobias Glasmachers. 2018. Challenges in High-Dimensional Reinforcement Learning with Evolution Strategies. In *Parallel Problem Solving from Nature - PPSN XV - 15th International Conference, Coimbra, Portugal, September 8-12, 2018, Proceedings, Part II*. 411–423. https://doi.org/10.1007/978-3-319-99259-4_33
- [34] Sharan Narang, Gregory Diamos, Shubho Sengupta, and Erich Elsen. 2017. Exploring Sparsity in Recurrent Neural Networks. In *International Conference on Learning Representations*.
- [35] Daiyi Peng, Xuanyi Dong, Esteban Real, Mingxing Tan, Yifeng Lu, Gabriel Bender, Hanxiao Liu, Adam Kraft, Chen Liang, and Quoc Le. 2020. PyGlove: Symbolic Programming for Automated Machine Learning. In *Advances in Neural Information Processing Systems 33: Annual Conference on Neural Information Processing Systems 2020, NeurIPS 2020, December 6-12, 2020, virtual*. <https://proceedings.neurips.cc/paper/2020/hash/012a91467f210472fab4e11359bbfef6-Abstract.html>
- [36] Hieu Pham, Melody Y. Guan, Barret Zoph, Quoc V. Le, and Jeff Dean. 2018. Efficient Neural Architecture Search via Parameter Sharing. In *Proceedings of the 35th International Conference on Machine Learning, ICML 2018, Stockholm, Sweden, July 10-15, 2018*. 4092–4101. [arXiv:1802.01548](https://arxiv.org/abs/1802.01548) <http://arxiv.org/abs/1802.01548>
- [37] Esteban Real, Alok Aggarwal, Yanping Huang, and Quoc V. Le. 2018. Regularized Evolution for Image Classifier Architecture Search. *CoRR* abs/1802.01548 (2018). [arXiv:1802.01548](https://arxiv.org/abs/1802.01548) <http://arxiv.org/abs/1802.01548>
- [38] Esteban Real, Chen Liang, David R. So, and Quoc V. Le. 2020. AutoML-Zero: Evolving Machine Learning Algorithms From Scratch. *CoRR* abs/2003.03384 (2020). [arXiv:2003.03384](https://arxiv.org/abs/2003.03384) <https://arxiv.org/abs/2003.03384>
- [39] D. E. Rumelhart. 1987. Personal Communication. *Princeton* (1987).
- [40] Tim Salimans, Jonathan Ho, Xi Chen, Szymon Sidor, and Ilya Sutskever. 2017. Evolution Strategies as a Scalable Alternative to Reinforcement Learning. *arXiv* abs/1703.03864 (2017).
- [41] John Schulman, Filip Wolski, Prfulla Dhariwal, Alec Radford, and Oleg Klimov. 2016–2018. Proximal policy optimization algorithms. *arXiv preprint arXiv:1707.06347* (2016–2018).
- [42] Abigail See, Minh-Thang Luong, and Christopher D. Manning. 2016. Compression of Neural Machine Translation Models via Pruning. In *Proceedings of The 20th SIGNLL Conference on Computational Natural Language Learning*. Association

- for Computational Linguistics, Berlin, Germany.
- [43] David R. So, Quoc V. Le, and Chen Liang. 2019. The Evolved Transformer. In *Proceedings of the 36th International Conference on Machine Learning, ICML 2019, 9-15 June 2019, Long Beach, California, USA*. 5877–5886. <http://proceedings.mlr.press/v97/so19a.html>
 - [44] Xingyou Song, Wenbo Gao, Yuxiang Yang, Krzysztof Choromanski, Aldo Pacchiano, and Yunhao Tang. 2020. ES-MAML: Simple Hessian-Free Meta Learning. In *8th International Conference on Learning Representations, ICLR 2020, Addis Ababa, Ethiopia, April 26-30, 2020*. <https://openreview.net/forum?id=S1exA2NtDB>
 - [45] Xingyou Song, Yiding Jiang, Stephen Tu, Yilun Du, and Behnam Neyshabur. 2020. Observational Overfitting in Reinforcement Learning. In *8th International Conference on Learning Representations, ICLR 2020, Addis Ababa, Ethiopia, April 26-30, 2020*. <https://openreview.net/forum?id=HJli2hNKDH>
 - [46] Xingyou Song, Yuxiang Yang, Krzysztof Choromanski, Ken Caluwaerts, Wenbo Gao, Chelsea Finn, and Jie Tan. 2020. Rapidly Adaptable Legged Robots via Evolutionary Meta-Learning. (2020). <https://arxiv.org/abs/2003.01239>
 - [47] Nitish Srivastava, Geoffrey Hinton, Alex Krizhevsky, Ilya Sutskever, and Ruslan Salakhutdinov. 2014. Dropout: A Simple Way to Prevent Neural Networks from Overfitting. *Journal of Machine Learning Research* 15 (2014), 1929–1958.
 - [48] Kenneth O. Stanley and Risto Miikkulainen. 2002. Evolving Neural Network through Augmenting Topologies. *Evolutionary Computation* 10, 2 (2002), 99–127.
 - [49] Rainer Storn and Kenneth V. Price. 1997. Differential Evolution - A Simple and Efficient Heuristic for global Optimization over Continuous Spaces. *J. Glob. Optim.* 11, 4 (1997), 341–359. <https://doi.org/10.1023/A:1008202821328>
 - [50] Mingxing Tan, Bo Chen, Ruoming Pang, Vijay Vasudevan, and Quoc V. Le. 2018. MnasNet: Platform-Aware Neural Architecture Search for Mobile. *CoRR abs/1807.11626* (2018). arXiv:1807.11626 <http://arxiv.org/abs/1807.11626>
 - [51] Mingxing Tan and Quoc V. Le. 2019. EfficientNet: Rethinking Model Scaling for Convolutional Neural Networks. In *Proceedings of the 36th International Conference on Machine Learning, ICML 2019, 9-15 June 2019, Long Beach, California, USA*. 6105–6114. <http://proceedings.mlr.press/v97/tan19a.html>
 - [52] Yujin Tang, Duong Nguyen, and David Ha. 2020. Neuroevolution of self-interpretable agents. In *GECCO '20: Genetic and Evolutionary Computation Conference, Cancún Mexico, July 8-12, 2020*. 414–424. <https://doi.org/10.1145/3377930.3389847>
 - [53] Emanuel Todorov, Tom Erez, and Yuval Tassa. 2012. MuJoCo: A physics engine for model-based control. In *2012 IEEE/RSJ International Conference on Intelligent Robots and Systems, IROS 2012, Vilamoura, Algarve, Portugal, October 7-12, 2012*. 5026–5033. <https://doi.org/10.1109/IROS.2012.6386109>
 - [54] Oriol Vinyals, Meire Fortunato, and Navdeep Jaitly. 2015. Pointer Networks. In *Advances in Neural Information Processing Systems 28: Annual Conference on Neural Information Processing Systems 2015, December 7-12, 2015, Montreal, Quebec, Canada*. 2692–2700.
 - [55] Colin White, Willie Neiswanger, and Yash Savani. 2019. BANANAS: Bayesian Optimization with Neural Architectures for Neural Architecture Search. *CoRR abs/1910.11858* (2019). arXiv:1910.11858 <http://arxiv.org/abs/1910.11858>
 - [56] Ronald J. Williams. 1992. Simple Statistical Gradient-Following Algorithms for Connectionist Reinforcement Learning. *Machine Learning* 8 (1992), 229–256. <https://doi.org/10.1007/BF00992696>
 - [57] Saining Xie, Alexander Kirillov, Ross B. Girshick, and Kaiming He. 2019. Exploring Randomly Wired Neural Networks for Image Recognition. *CoRR abs/1904.01569* (2019). arXiv:1904.01569
 - [58] Chris Ying, Aaron Klein, Eric Christiansen, Esteban Real, Kevin Murphy, and Frank Hutter. 2019. NAS-Bench-101: Towards Reproducible Neural Architecture Search. In *Proceedings of the 36th International Conference on Machine Learning, ICML 2019, 9-15 June 2019, Long Beach, California, USA*. 7105–7114. <http://proceedings.mlr.press/v97/ying19a.html>
 - [59] Haonan Yu, Sergey Edunov, Yuandong Tian, and Ari Morcos. 2019. Playing the lottery with rewards and multiple languages: lottery tickets in RL and NLP. *arXiv abs/1906.02768* (2019).
 - [60] Wenhao Yu, Jie Tan, Yunfei Bai, Erwin Coumans, and Sehoon Ha. 2020. Learning Fast Adaptation With Meta Strategy Optimization. *IEEE Robotics Autom. Lett.* 5, 2 (2020), 2950–2957. <https://doi.org/10.1109/LRA.2020.2974685>
 - [61] Barret Zoph and Quoc V. Le. 2017. Neural Architecture Search with Reinforcement Learning. In *5th International Conference on Learning Representations, ICLR 2017, Toulon, France, April 24-26, 2017, Conference Track Proceedings*.

APPENDIX

A NETWORK VISUALIZATIONS

A.1 Weight Sharing

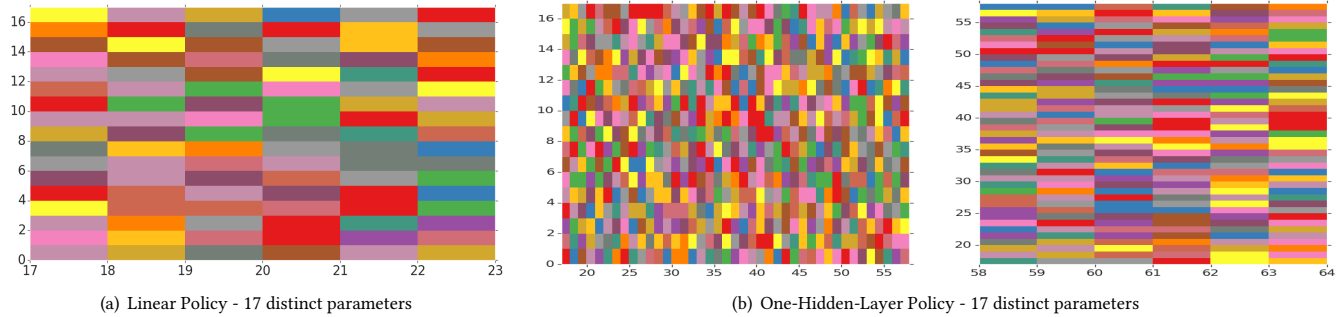


Figure 8: (a): Partitioning of edges into distinct weight classes obtained for the linear policy for HalfCheetah environment from OpenAI Gym. (b): Partitioning of edges for a policy with one hidden layer encoded by two matrices. State and action dimensionalities are: $s = 17$ and $a = 6$ respectively and hidden layer for the architecture from (b) is of size 41. Thus the size of the matrices are: 17×6 for the linear policy from (a) and: 17×41 , 41×6 for the nonlinear one from (b).

A.2 Edge Pruning

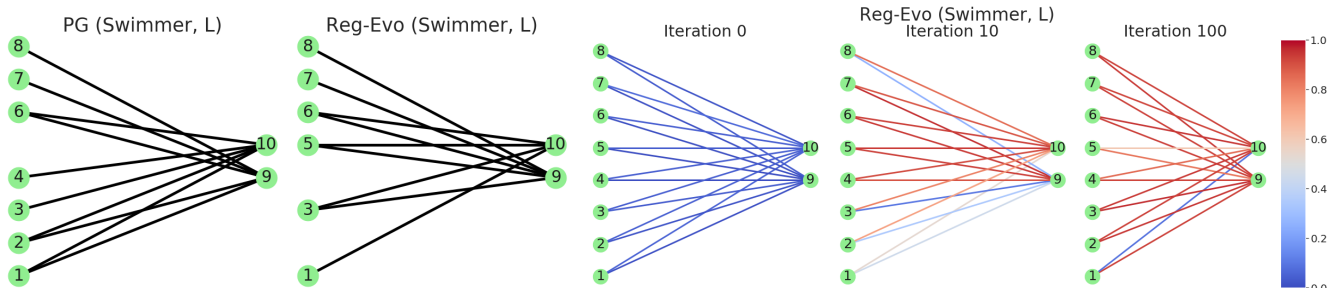


Figure 9: (Left) Final architectures that PG and Reg-Evo converged to on Swimmer with a linear (L) policy, as specified in Subsection 5.7. Note that the controller does not select all edges even if it is allowed in the boolean search space, but also ignores some state values. (Right): Convergence result for Reg-Evo, similar to Fig. 7 in Subsection 5.7.

B EXTENDED EXPERIMENTAL RESULTS

As standard in RL, we take the mean and standard deviation of the final rewards across 3 seeds for every setting. “L”, “H” and “H, H” stand for: linear policy, policy with one hidden layer, and policy with two such hidden layers respectively.

B.1 Baseline Method Comparisons

In terms of the masking baseline, while [26] fixes the sparsity of the mask, we instead initialize the sparsity at 50% and increasingly reward smaller networks (measured by the size of the mask $|m|$) during optimization to show the effect of pruning. Using this approach on several Open AI Gym tasks, we demonstrate that masking mechanism is capable of producing compact effective policies up to a high level of pruning. At the same time, we show significant decrease of performance at the 80-90% compression level, quantifying accurately its limits for RL tasks (see: Fig. 10).

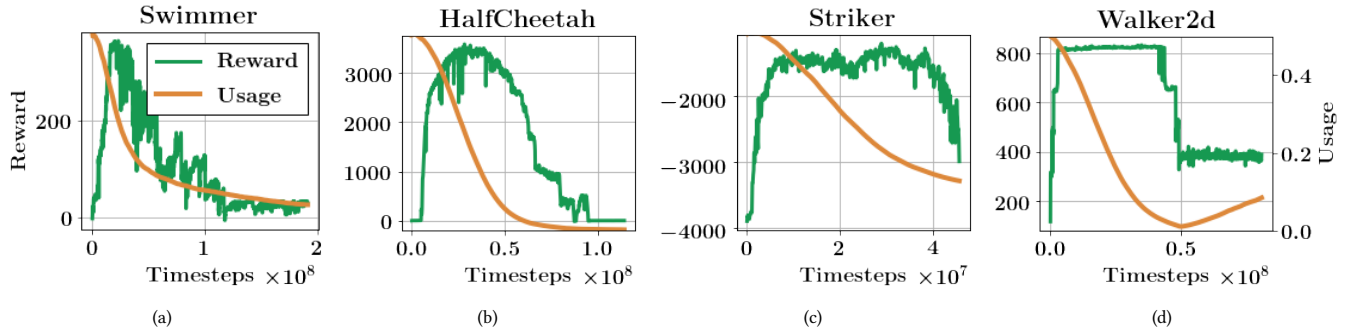


Figure 10: The results from training both a mask m and weights θ of a neural network with two hidden layers. ‘Usage’ stands for number of edges used after filtering defined by the mask. At the beginning, the mask is initialized such that $|m|$ is equal to 50% of the total number of parameters in the network.

B.2 Weight Sharing

Env.	Dim.	Arch.	Partitions	(PG, Reg-Evo, RS) Reward	Env.	Dim.	Arch.	Partitions	(PG, Reg-Evo, RS) Reward
Swimmer	(8,2)	L	8	(366 ± 0, 296 ± 31, 5 ± 1)	Swimmer	(8,2)	H	8	(361 ± 4, 362 ± 1, 15 ± 0)
Reacher	(11,2)	L	11	(−10 ± 4, −157 ± 62, −135 ± 10)	Reacher	(11,2)	H	11	(−6 ± 0, −23 ± 11, −157 ± 2)
Hopper	(11,3)	L	11	(2097 ± 788, 1650 ± 320, 16 ± 0)	Hopper	(11,3)	H	11	(3288 ± 119, 2834 ± 75, 95 ± 2)
HalfCheetah	(17,6)	L	17	(2958 ± 73, 3477 ± 964, 129 ± 183)	HalfCheetah	(17,6)	H	17	(4258 ± 1034, 4894 ± 110, −41 ± 5)
Walker2d	(17,6)	L	17	(326 ± 86, 2079 ± 1085, 8 ± 0)	Walker2d	(17,6)	H	17	(1684 ± 1008, 2026 ± 46, −5 ± 1)
Pusher	(23,7)	L	23	(−68 ± 2, −198 ± 76, −503 ± 4)	Pusher	(23,7)	H	23	(−225 ± 131, −350 ± 236, −1049 ± 40)
Striker	(23,7)	L	23	(−247 ± 11, −376 ± 149, −590 ± 18)	Striker	(23,7)	H	23	(−992 ± 2, −466 ± 238, −1009 ± 1)
Thrower	(23,7)	L	23	(−819 ± 8, −1555 ± 427, −12490 ± 708)	Thrower	(23,7)	H	23	(−1873 ± 690, −818 ± 363, −12847 ± 172)

Table 3: Results via weight sharing across PG, Reg-Evo, and random search controllers. The number of partitions is always set to be $\max(|\mathcal{S}|, |\mathcal{A}|)$.

B.3 Edge Pruning

Env.	Dim.	Arch.	(PG, Reg-Evo, RS) Reward
Swimmer	(8,2)	H	(105 ± 116, 343 ± 2, 21 ± 1)
Reacher	(11,2)	H	(−16 ± 5, −52 ± 5, −160 ± 2)
Hopper	(11,3)	H	(3349 ± 206, 2589 ± 106, 66 ± 0)
HalfCheetah	(17,6)	H	(2372 ± 820, 4016 ± 726, −156 ± 22)
Walker2d	(17,6)	H	(3813 ± 128, 1847 ± 710, 0 ± 2)
Pusher	(23,7)	H	(−133 ± 31, −156 ± 17, −503 ± 15)
Striker	(23,7)	H	(−178 ± 54, −130 ± 16, −464 ± 13)
Thrower	(23,7)	H	(−532 ± 29, −1107 ± 158, −7797 ± 112)

Table 4: Results via weight sharing across PG, Reg-Evo, and random search controllers. The number of edges is always set to be 64 in total, or (32, 32) across the two weight matrices when using a single hidden layer.

B.4 Edge Pruning + Nonlinearity Search

Env.	Dim.	Arch.	(PG, Reg-Evo, RS) Reward
Swimmer	(8,2)	H	(247 ± 110, 359 ± 5, 11 ± 3)
Hopper	(11,3)	H	(2270 ± 1464, 57 ± 7)
HalfCheetah	(17,6)	H	(3028 ± 469, 5436 ± 978, −268 ± 29)
Walker2d	(17,6)	H	(1057 ± 413, 2006 ± 248, 0 ± 1)

Table 5: Results using the same setup as Table 4, but allowing nonlinearity search.

C EXACT SETUP AND HYPERPARAMETERS

C.1 Controller Setups

C.1.1 Regularized Evolution. We use uniform sampling, with the tournament size as \sqrt{n} where n is the number of workers (which is defaulted to 150; see: "ES Algorithm" subsection). This is also recommended in [37].

C.1.2 Policy Gradient. We use a gradient update batch size of 64 to the Pointer Network, while using PPO as the policy gradient algorithm, with its default (recommended) hyperparameters from [35].

C.2 Policy

By default, unless specified, we use Tanh non-linearities with 32 units for each hidden layer. We use the following default hyperparameters for the following search spaces:

C.2.1 Weight Sharing. The number of partitions (or "colors") is set to $\max(|\mathcal{S}|, |\mathcal{A}|)$. This is both in order to ensure a linear number of trainable parameters compared to the quadratic number for unstructured networks, as well as allow sufficient parameterization to deal with the entire state/action values.

C.2.2 Edge Pruning. We collect all possible edges from a normal neural network into a pool E_{max} and set $|E| = 64$ as the number of distinct choices, passed to the `pyglove.manyof`. Similar to weight sharing, this choice is based on the value $\max(|\mathcal{S}|, H)$ or $\max(|\mathcal{A}|, H)$, where $H = 32$ is the number of hidden units, which is linear in proportion to respectively, the maximum number of weights $|\mathcal{S}| \cdot H$ or $|\mathcal{A}| \cdot H$. Since a hidden layer neural network has two weight matrices due to the hidden layer connecting to both the state and actions, we thus have ideally a maximum of $32 + 32 = 64$ edges.

C.2.3 Nonlinearity Search. We use the same nonlinearity choices found in [16]. These are: {Tanh, ReLU, Exp, Identity, Sin, Sigmoid, Absolute Value, Cosine, Square, Reciprocal, Step Function.}

C.3 Environment

For all environments, we set the horizon $T = 1000$. We also use the reward without alive bonuses for weight training as commonly used [30] to avoid local maximum behaviors (such as an agent simply standing still to collect a total of 1000 reward), but report the final score as the real reward with the alive bonus.

C.4 ES Algorithm

For all environments, we used reward normalization and state normalization implemented from [31]. We set smoothing parameter $\sigma = 0.1$ and step size $\eta = 0.01$. Unless specified, we use 150 workers, where 100 are used for perturbations in the antithetic case (and thus $100 / 2 = 50$ distinct perturbations are used) and 50 more are used for evaluation on the current parameter settings.

C.5 Baseline Details

We consider Unstructured, Toeplitz, Circulant and a masking mechanism [5, 26]. We introduce their details below. Notice that all baseline networks share the same general (1-hidden layer, Tanh nonlinearity) architecture from C.2. This implies that we only have two weight matrices $W_1 \in \mathbb{R}^{|\mathcal{S}| \times h}$, $W_2 \in \mathbb{R}^{h \times |\mathcal{A}|}$ and two bias vectors $b_1 \in \mathbb{R}^h$, $b_2 \in \mathbb{R}^{|\mathcal{A}|}$, where $|\mathcal{S}|$, $|\mathcal{A}|$ are dimensions of state/action spaces. These networks differ in how they parameterize the weight matrices. We have:

C.5.1 Unstructured. A fully-connected layer with unstructured weight matrix $W \in \mathbb{R}^{a \times b}$ has a total of ab independent parameters.

C.5.2 Toeplitz. A toeplitz weight matrix $W \in \mathbb{R}^{a \times b}$ has a total of $a + b - 1$ independent parameters. This architecture has been shown to be effective in generating good performance on benchmark tasks yet compressing parameters [5].

C.5.3 Circulant. A circulant weight matrix $W \in \mathbb{R}^{a \times b}$ is defined for square matrices $a = b$. We generalize this definition by considering a square matrix of size $n \times n$ where $n = \max\{a, b\}$ and then do a proper truncation. This produces n independent parameters.

C.5.4 Masking. One additional technique for reducing the number of independent parameters in a weight matrix is to mask out redundant parameters [26]. This slightly differs from the other aforementioned architectures since these other architectures allow for parameter sharing while the masking mechanism carries out pruning. To be concrete, we consider a fully-connected matrix $W \in \mathbb{R}^{a \times b}$ with ab independent parameters. We also setup another mask weight $\Gamma \in \mathbb{R}^{a \times b}$. Then the mask is generated via

$$\Gamma' = \text{softmax}(\Gamma/\alpha)$$

where `softmax` is applied elementwise and α is a constant. We set $\alpha = 0.01$ so that the softmax is effectively a thresholding function with outputs near binary masks. We then treat the entire concatenated parameter $\theta = [W, \Gamma]$ as trainable parameters and optimize both using ES methods. Note that this softmax method can also be seen as an instance of the continuous relaxation method from DARTS [28]. At convergence, the effective number of parameter is $ab \cdot \lambda$ where λ is the proportion of Γ' components that are non-zero. During optimization,

we implement a simple heuristics that encourage sparse network: while maximizing the true environment return $f(\theta) = \sum_{t=1}^T r_t$, we also maximize the ratio $1 - \lambda$ of mask entries that are zero. The ultimate ES objective is: $f'(\theta) = \beta \cdot f(\theta) + (1 - \beta) \cdot (1 - \lambda)$, where $\beta \in [0, 1]$ is a combination coefficient which we anneal as training progresses. We also properly normalize $f(\theta)$ and $(1 - \lambda)$ before the linear combination to ensure that the procedure is not sensitive to reward scaling.